Trop J Nat Prod Res, November 2023; 7(11):5087-5096

ISSN 2616-0684 (Print)
ISSN 2616-0692 (Electronic)

Tropical Journal of Natural Product Research

Available online at https://www.tjnpr.org

Original Research Article

Molecular Docking and Dynamics Study of Compounds from *Combretum indicum* var. B Seeds as Alcohol Dehydrogenase Inhibitors

Samsul Hadi[1]*, Deni Setiawan[1], Pratika Viogenta[1], Sunardi Sunardi[2], Kunti Nastiti[3], Khoirun Nisa[4], Dicky Andiarsa[5]

[1]*Department of Pharmacy, Faculty of Mathematics and Natural Sciences, Lambung Mangkurat University Banjarbaru, South Kalimantan, Indonesia*
[2]*Department of Chemistry, Faculty of Mathematics and Natural Sciences, Lambung Mangkurat University Banjarbaru, South Kalimantan, Indonesia*
[3]*Department of Pharmacy, Faculty of Health, Sari Mulia University*
[4]*Research Centre for Food Technology and Processing - The National Research and Innovation Agency (BRIN), 55861, Yogyakarta, Indonesia*
[5]*Research Organization for Health, The National Research and Innovation Agency Republic of Indonesia (BRIN), 40135, Bogor, Indonesia*

ARTICLE INFO

Article history:
Received 10 August 2023
Revised 11 October 2023
Accepted 19 October 2023
Published online 01 December 2023

ABSTRACT

Ethylene glycol is one of the causes of acute kidney failure due to the metabolic byproducts produced on its metabolism by the enzyme alcohol dehydrogenase (ADH) in the liver. Therefore, this study is aimed at identifying potential compounds from *Combretum indicum* var B seeds that can inhibit ADH enzyme. The seeds of *Combretum indicum* var B were extracted by maceration in ethanol, the constituents of the extract was analysed by LC-MS (Liquid Chromatography-Mass Spectrometry). The alcohol dehydrogenase inhibitory activity of the identified compounds was investigated *in silico* via molecular docking and dynamics study. Their potential for oral use was also investigated using the SwissADME and admetSAR software. The results of the LC-MS analysis identified seventeen (17) compounds in the seeds of *Combretum indicum*. The molecular docking and dynamics results showed that six (6) of the compounds, namely; 9,10-Dihydrophenanthrene, 2,3-Dihydroxy-3',4,4',5-tetramethoxybibenzyl, 2-Hydroxy-3,4,6,7-tetramethoxy-9,10-dihydro phenanthrene, 3-Hydroxy-2,4,6,7-tetramethoxy-9,10 dihydrophenanthrene, Erythrophyllic acid, and 3'-Hydroxy-3,4,4'5-tetramethoxystilbene has high binding energy. These compounds exhibited better binding energy than the standard ligand (fomepizole) - a known inhibitor of ADH. Therefore, these compounds could serve as potential inhibitors of alcohol dehydrogenase with better activity than the standard ligand.

***Keywords*:** Ethylene glycol, Alcohol dehydrogenase, *Combretum indicum*, Seeds.

Introduction

Acute kidney damage is increasingly gaining attention in recent times, especially in children. As the death rate keeps rising, prompt preventive measure is required. The National Kidney Foundation (NKF) data shows that 10% of human population has acute kidney failure.[1] According to WHO, about 66 children in the Gambia died due to the consumption of paracetamol syrup contaminated with ethylene glycol.[2] In Indonesia, the data from the Ministry of Health shows that up to 325 cases of acute kidney failure in children was recorded in December 2022. These cases were distributed across 27 provinces, with a 52% mortality rate.[3] Ethylene glycol present in paediatric syrup is thought to be the major cause of acute renal failure, although, explanation for the present increase in the number of cases is still unknown.[4] To avoid more severe cases of kidney failure, the Indonesian government has taken some proactive measures through a recall of all syrups containing ethylene glycol.[4]
Exposure to ethylene glycol causes severe kidney damage due to its metabolic byproducts. Ethylene glycol is metabolized in the liver by alcohol dehydrogenase (ADH) to glycolic and oxalic acids.

*Corresponding author. E mail: samsul.hadi@ulm.ac.id
Tel: +6283152962036

Citation: Hadi S, Setiawan D, Viogenta P, Sunardi S, Nastiti K, Nisa K, Andiarsa D. Molecular Docking and Dynamics Study of Compounds from *Combretum indicum* var. B Seeds as Alcohol Dehydrogenase Inhibitors. Trop J Nat Prod Res. 2023; 7(11):5087-5096. http://www.doi.org/10.26538/tjnpr/v7i11.11

Official Journal of Natural Product Research Group, Faculty of Pharmacy, University of Benin, Benin City, Nigeria

Oxalic acid reacts with calcium to produce oxalic acid monohydrate (water-insoluble).[5] Oxalic acid monohydrate is retained in the tubules and causes renal irritation. Acute tubular damage results as a result of nephrotoxic compounds which affect the kidney's ability to transport, process, and excrete drugs.[6] An approach in the treatment of acute kidney failure due to ethylene glycol is the use of fomepizole and ethanol, which are competitive inhibitors of ADH.[7] Due to the significant variation in the elimination process, including the cost of fomepizole and the difficulty in maintaining therapeutic concentration of ethanol, numerous alternative therapies have continued to evolve.[8] An approach which involves the *in silico* identification of compounds that can serve as potential inhibitors of ADH was employed in this study.
Combretum, particularly *Combretum indicum* L. var. B (also known as *Quisqualis indica* L.), is a plant frequently used to treat liver diseases. Several species of the genus Combretum have been studied and found to possess hepatoprotective properties. [9–13] For instance, the water extract of *Combretum dolichopentalum* leaves have been found to protect liver cells from CCl_4 – induced hepatic damage.[14] *Combretum sericeum* root water extract have also been shown to protect the liver from paracetamol-induced hepatic damage, and caused a decrease in alanine transminase (ALT), aspartate aminotransferase (AST), alkaline phosphatase (ALP), creatinine (CRT), urea, cholesterol, and triacylglycerol as well as an increased levels of superoxide dismutase (SOD), catalase (CAT), and thiobarbituric acid reactive substances (TBARS).[15] Similarly, *Combretum albidum* has also shown hepatoprotective ability against CCl_4- induced toxicity by reducing the levels of ALT, AST, ALP, total bilirubin (TB), and TBARS, and antioxidants activity by increasing levels of reduced glutathione (GSH), superoxide dismutase (SOD), catalase (CAT), glutathione peroxidase (GPx), glutathione-s-transferase (GST), and total protein (TP).[13] The water extract of *Combretum micranthum* leaves also have

 ISSN 2616-0684 (Print)
ISSN 2616-0692 (Electronic)

hepatoprotective effect against paracetamol-induced toxicity.[10] Methanol and water extracts of *Combretum quadrangulare* have shown the potential to prevent D-GalN/TNF-alpha-induced hepatocyte death.[16] Ethanol extract from the roots of *Combretum hypopilinum* has also shown hepatoprotection against CCl_4-induced liver damage through antioxidants and anti-inflammatory mechanisms.[17] Furthermore, the compounds; 1-*O*-Galloyl-6-*O*-(4-hydroxy-3,5-dimethoxy)benzoyl-beta-D-glucose, (-)-epicatechin, 2*α*,6*β*-dihydroxybethulinic acid, 6*β*-hydroxyhovenic acid oleanane type, and 6*β*-hydroxyarjunic acid, which were isolated from *Combretum quadrangulare* have been found to have hepatoprotective activity against D-GalN/TNF-alpha-induced damage in primary cultured rat hepatocytes.[18]

Molecular docking studies of potential inhibitors of ADH are still in their infancy. For example, hypophyllanthin, gallic acid, and phyllanthin are few compounds lwith high binding affinity with ADH enzyme.[19] In addition, rutin has been shown to form a stable complex with ADH via hydrogen and Van der Waals bonds interaction at the valine (VAL) residue.[20] Differences in the binding energy and stability of ADH-ligand complex has been observed depending on the source. For example, the ADH from ethanol-producing yeast mutant strain *Pichia kudriavzevii* BGY1-γm produce a protein-ligand complex that is stable with low binding energy,[21] the ADH from *Synechocystis* sp. PCC 6803 has more active/binding sites than the ADH from horse liver.[22]

Based on the foregoing, the genus *Combretum* could be a potential source of hepatoprotective compounds with alcohol dehydrogenase inhibitory activity. It is worthy to note that alcohol dehydrogenase (ADH) inhibitory activity has not been carried out on *Combretum indicum* var. B. Therefore, the present study is undertaken with the aim of identifying the compounds from *Combretum indicum* var. B seeds that could have potential alcohol dehydrogenase inhibitory activity using *in silico* approach.

Materials and Methods

Solvents and chromatographic materials

Ethanol (96%), methanol p.a (Merck), water (Merck), formic acid (Merck), Hypersil GOLD™ C-18 (Thermo Scientific™), and 0.2µm, 28 mm Syringe Filter (AXIVA).

Equipment and software

The tools used included Thermo HPLC-DIONEX ULTIMATE -TSQ Quantum Access MAX Triple Quadrupole Mass Spectrometer (UltiMate 3000, Thermo Fisher Scientific, Waltham), MS-DIAL library (4.9.221218), syringe filter (Filstar, Starlab, Hawach), Yasara (21.6.2), discovery studio (4.5), Swissadme (http://www.swissadme.ch/), admeTSAR 2.0 (http://lmmd.ecust.edu.cn/admetsar1/), and AutoDock (4.2).

Collection and identification of plant material

Combretum indicum var. B seeds were collected from Tanah Bumbu, South Kalimantan (cordinate number -3.720130 115.617257) on 2nd February, 2023. The plant material was identified by Dr. Gunawan, a plant taxonomist at the Department of Biology, Lambung Mangkurat University, *Banjarbaru, South Kalimantan, Indonesia*. Herbarium specimen with the determination number 032/LB.LABDASAR/II/2022 and herbarium collection number XII-21-018-S was deposited.

Plant Extraction and LC-MS Analysis

Combretum indicum var. B seeds (50 g) were macerated with 5 L of 96% ethanol. The extract was concentrated by evaporation over a water bath (WNB 22 w/5rack, Memmert, Germany) at 60°C. A total of 10 milligrams of the concentrated extract was dissolved in 10 mL of methanol, and the solution was filtered using a 0.22 µm syringe filter (Filstar, Starlab, Hawach). The injection volume was 5 µL, and the MS read mode covered the range of 150 to 1000 Da. Water:formic Acid 0.1% and MeOH:formic Acid 0.1% were used as the mobile phase in a gradient elution of 95%:5% to 5%:95% at a flow rate of 0.3 mL/min. Mass spectrometric analysis of the separated compounds was done using MS-DIAL.

Protein preparation

Alcohol dehydrogenase enzyme was crystallized from horse liver with code 1HLD (Horse liver alcohol dehydrogenase).[23] The enzyme's structure was reduced with NAD^+ complexation and 2,3,4,5,6-pentafluorobenzyl alcohol. This complex was obtained using X-rays at 4°C, data on a single triclinic crystal (unit cell dimensions: a = 52.3 Å, b = 44.5 Å, c = 93.9 Å, a = 104.7"; p = 102.2"; and y = 70.6") were collected using a multiwire area detector (Nicolet) from Xentronics mounted on a rotating anode from Rigaku with 0.1" oscillation frames (Daresbury, England) at 2.1 Å resolution and a monoclinic form (P2 (1)) refinement value of 18.3% and a triclinic crystalline form refinement value of 18.9% at a resolution of 2.4 Å. During this process, water and ligands not involved in the interaction were removed, leaving protein, NAD, and Zn. The protein chains used were refined using the Yasara program to assemble the missing residues.[24]

Ligand screening

Ligand screening was conducted using SWISSADME (www.swissadme.ch/) to determine the similarity of compounds from *Combretum indicum* seeds with existing oral drugs based on the Lipinski rule.[25–27] To make the selection, a maximum molecular weight limit of 500 Da was applied, the number of H acceptors was less than 10, the number of H donors was less than 5, and MLog P < 4.15. Subsequently, a selection was made using ADMETSAR (lmmd.ecust.edu.cn/admetsar2) with the HIA (Human intestinal absorption) and Human oral bioavailability (HO) indicators. When the values of these two parameters are positive, it indicate that the compounds will be well absorbed and possess good bioavailability.

Molecular Docking

Molecular docking was done using AutoDock4 with the Lamarckian Genetic and Rigid docking mode algorithm.[28] The docking was carried out by running 100 ligand conformations to obtain the best pose of the ligand when interacting with the enzyme alcohol dehydrogenase with code 1HLD. As there was no active ligand in IHLD crystals, it was necessary to predict the active site using CASTp (sts.bioe.uic.edu/castp/calculation.html). The data obtained from the docking were Binding energy (kcal/mol) and Dissociation constant (pM).

Molecular dynamics simulation

Molecular dynamics study was done using the Yasara program. The program settings included optimized hydrogen bonding to boost the stability of dissolved ligands and pKa prediction to improve the protonation of protein residues. The chosen pH was the physiological pH of the body. NaCl ions were added at a concentration of 0.9%, followed by Na and Cl ions to normalize cell conditions. The simulation was carried out at a temperature of 310K, with a density of water of 0.997 g/mL. The cell shape was cuboidal, and the cell boundaries were periodic, with a cell elongation of 10 Å on each side next to the solvent. To prevent the solute from spreading and going over the periodic border, storage correction was activated. The simulation was ran for 100 ns with AMBER14 force field applied to the solute after the steepest descent and minimizations produced by simulating annealing to eliminate conflicts. The data obtained from molecular dynamics were RMSD (root-mean-square deviation), Rg (Radius of gyration), RMSF (root mean square fluctuation), SASA (solvent-accessible-surface-area), Hydrogen bond, and binding energy. The PBS (Poisson-Boltzmann method) without entropy (standard mode analysis) was employed by the Yasara program. More positive binding energy suggested greater interactions between molecules, according to Yasara standards.[29] The equation used was;

Binding energy (i) = [epotrec (i) + esolrec (i) + epotlig + esollig] – [epotcmp (i) + esolcmp (i)]

Where i is the position number, epot is the potential energy for the complex (epotcmp), free protein (epotrec), or free ligand (epotlig), and esol is the solvation energy for the complex (esolcmp), free protein (esolrec), or free ligand (esollig).

ISSN 2616-0684 (Print)
ISSN 2616-0692 (Electronic)

Results and Discussion

LC-MS/MS analysis

From the LC-MS/MS analysis, seventeen (17) compounds were identified in *Combretum indicum* var. B seeds as shown in Table 1 and Figure 1. In this analysis, there were no fractions of the masses of the parent ions because an electrospray ionization was used, resulting in the appearance of only the parent peaks which are the same as that obtained with GC-MS.[30]

Protein preparation

Based on the refinement carried out, the following energy values were obtained: -97757.24 kJ/mol, Dihedrals: 1.99, Packing 1D: -0.33, Packing 3D: -0.47, Average: 0.40. These values indicated that the protein conformation occupied the lowest energy and was stable.[31] Based on CASTp, the active site of 1HLD was Area (SA): 582,879 Å, and Volume (SA): 326,273 Å. The residue involved in the interaction was SER48, LEU57, HIS67, PHE93, LEU116, PHE140, LEU141, CYS174, ILE318, PHE319, ZN375, and NAD801 as shown in Figure 2.

Protein preparation involved Zn and NAD due to the mechanism of action of alcohol dehydrogenase enzyme in converting ethylene glycol substrate to glycol aldehyde, glycol oxalic acid, and finally forming oxalic acid, involving the reduction of NAD^+ to NADH.[32] Oxalic acid is responsible for the acute kidney failure in children[33] and the initial inflammation.[34]

Ligand screening

The SWISS ADME screening results were presented in S1, while ADMETSAR screening results were shown in S2. The final results of the screening are summarized in Table 2 and Figure 3. The choice of per oral screening is due to the ease of use of the oral route, its safety compared to other routes such as injection (risk of infection or trauma to the skin), and easier long-term use and does not interfere with daily activities.[35]

Docking

The ligand was abbreviated as UNL1, representing one of three ligands involved in the interaction: the test ligand, Zn, and NAD. Based on the docking results obtained (Table 3), the compounds present in *Combretum indicum* var. B seeds exhibited superior binding energy compared to the standard ligang fomepizole (Pubchem CID 3406).

In the initial screening using the complex docking method, the compounds that bind to PHE93 residue were; 2,3-Dihydroxy-3',4,4',5-tetramethoxybibenzyl, 2-Hydroxy-3,4,6,7-tetramethoxy-9,10-dihydrophenanthrene, and 3'-Hydroxy-3,4,4'5-tetramethoxystilbene. The binding energy data indicated that six of the docked ligands have better binding energy compared to fomepizole in the order; 3'-Hydroxy-3,4,4'5-tetramethoxystilbene (-5.77 kcal/mol), 9,10-Dihydrophenanthrene (-6.54 kcal/mol), 2,3-Dihydroxy-3',4,4',5-tetramethoxybibenzyl (-6.65 kcal/mol), 3-Hydroxy-2,4,6,7-tetramethoxy-9,10-dihydrophenanthrene (-7.07 kcal/mol), 2-Hydroxy-3,4,6,7- tetramethoxy-9,10-dihydrophenanthrene (-7.28 kcal/mol) and Erythrophyllic acid (-7.52 kcal/mol) (Table 3 and Figure 4).

Additionally, the dissociation energies of the compounds were lower when they bind to the alcohol dehydrogenase enzyme, indicating their potential as inhibitors. These three compounds may eventually occupy the active site; however docking only produced one optimal pose, making it difficult to make a final choice. This study continued with molecular dynamics to study the stability of the complex between the enzyme and compounds. The molecular dynamics helped to validate the docking results. Based on molecular dynamics, all ligands that interacted with alcohol dehydrogenase showed stability without any significant fluctuations.

Molecular dynamics

From the molecular dynamics study carried out, the following parameters were obtained; RSMD Cα (Root Mean Square Deviation carbon alpha), RMSF (Root mean square fluctuation), SASA (Solvent-accessible surface area), Rg (Radius of gyration), Hydrogen bond, and Binding energy (Figure 5). RMSD Cα represented a fluctuation in protein conformation before and after interacting with ligands, indicating protein stability.[36] In this study, the alcohol dehydrogenase enzyme exhibited a mean RMSD of 2.078 Å, with the highest value of 2.514 Å. When this enzyme binds to fomepizole, there was an increase in RMSD value to 3.34 Å at 99 ns with a mean value of 2.258 Å. On binding to 9,10-Dihydrophenanthrene, RMSD increased to 2.812 Å at 77.3 ns with a mean value of 2.02 Å (Figure 5A). When bound to 2,3-Dihydroxy-3',4,4',5-tetramethoxybibenzyl, the highest RMSD 2.445 Å at 52.5 ns with a mean value of 1.984 Å. When it binds to 2-Hydroxy-3,4,6,7- tetramethoxy-9,10-dihydrophenanthrene, maximum RMSD of 2.669 Å was obtained at 53.1 ns with a mean of 2.113 Å. The ADH - 3-Hydroxy-2,4,6,7- tetramethoxy-9,10-dihydrophenanthrene complex exhibited the highest RMSD of 2.626 Å at 44.3 ns with a mean of 2.071 Å. The enzyme - Erythrophyllic acid complex had a maximum RMSD of 2.952 Å at 55.7 ns with a mean of 2.25 Å, while the enzyme complexed with 3'-Hydroxy-3,4,4'5-tetramethoxystilbene had it maximum RMSD at 52.8 ns with a mean of 2.504 Å. All ligands that bound to the enzyme had a change in RMSD value below 2 Å, indicating that the alcohol dehydrogenase enzyme-ligands complexes were stable.[37]

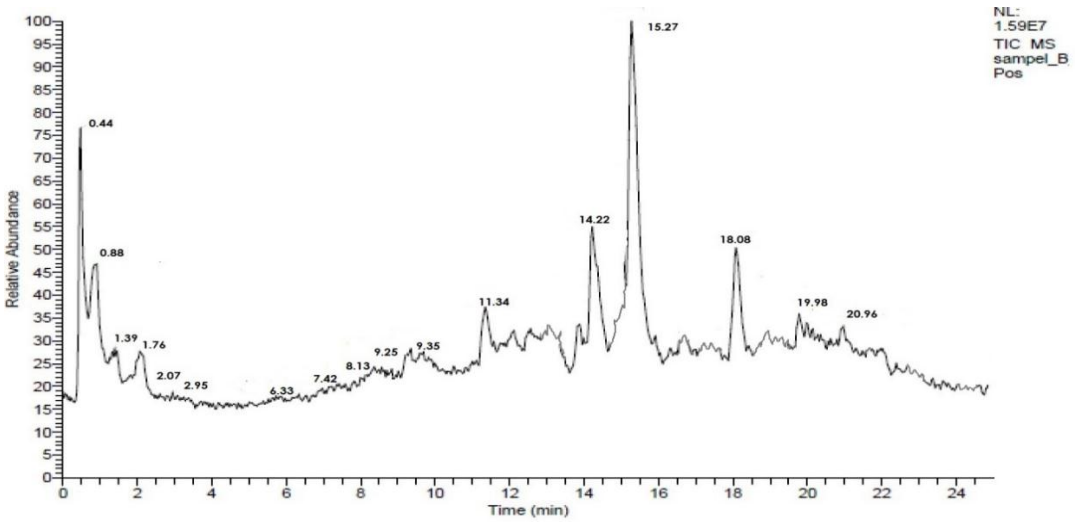

Figure 1: LC Chromatogram of ethanol extract of *Combretum indicum* var B seeds

ISSN 2616-0684 (Print)
ISSN 2616-0692 (Electronic)

RMSF analysis showed residual flexibility over a 100 ns simulation, with fluctuations above 3 Å, indicating changes in bonds between residues.[38] Fluctuations on the active site only occurred during the interaction between fomepizole and enzyme at residue LEU116 (Figure 5B). Meanwhile, the other changes did not affect the ligand - protein bond because they were outside the active site. Fluctuations beyond this active site occurred in the; (i) interaction of fomepizole with the enzyme at residues LYS113, ASN114, ASP115, LEU116, SER117, MET118, ASP297, SER298, GLN299, ASN300, LEU301, SER302, MET303, ASN304, MET 306, (ii) interaction of 9,10-Dihydrophenanthrene with enzyme at residues PRO296, ASP297, SER298, GLN299, ASN300, LEU301, SER302, ASN304, (iii) interaction of 3-Hydroxy-2,4,6,7- tetramethoxy-9,10-dihydrophenanthrene with enzyme at residues SER 298, LEU301, SER302, and (iv) interaction of 3'-Hydroxy-3,4,4'5-tetramethoxystilbene with enzyme at residues LYS 113, PRO296.

SASA described the character of the solvent for the ligand-enzyme complex, where increasing value indicated more accessible solvent with a quick access to the binding site.[39] From the results of the study as shown in Figure 5C, the enzyme SASA value was 15522.11 Å, increasing SASA values were observed for enzyme - fomepizole complex (16003.19 Å), enzyme - 9,10-Dihydrophenanthrene complex (15576.46 Å), enzyme - 3-Hydroxy-2,4,6,7- tetramethoxy-9,10-dihydrophenanthrene complex (15745.14 Å), enzyme - Erythrophyllic acid complex (15985.84 Å), and enzyme - 3'-Hydroxy-3,4,4'5-tetramethoxystilbene complex (15753.72 Å). However, some SASA values decreased for the enzyme-ligand complex compared to the unbound enzyme, these include enzyme - 2,3-Dihydroxy-3',4,4',5-tetramethoxybibenzyl complex (15397.33 Å), and enzyme - 2-Hydroxy-3,4,6,7- tetramethoxy-9,10-dihydrophenanthrene complex (15518.94 Å).

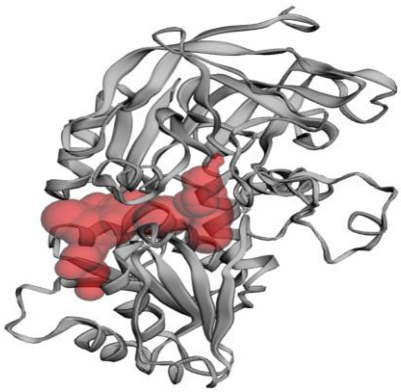

Figure 2: Active site prediction using CASTp (The red color is the active site of 1HLD)

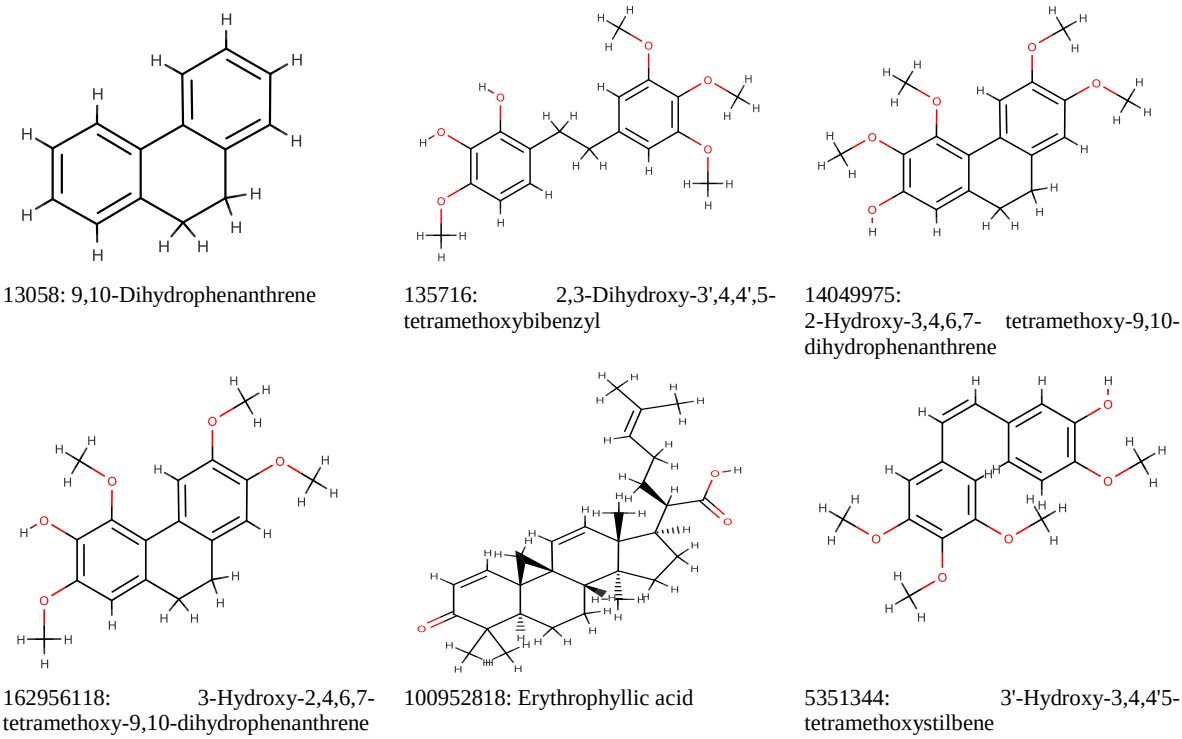

Figure 3: Chemical structures of the six selected compounds and their PubChem CID codes

Table 1: Compounds identified from the LC-MS analysis of *Combretum indicum* var B seeds ethanol extract

No	Rt	M+H	M-H	M	Compound
1	0.44	-	387.47	388.11	Combretol.[18]
2	0.88	181.17	179.24	180.09	9,10-Dihydrophenanthrene.[53]
3	1.39	-	243.08	244.10	3,4'-Dihydroxy-5-methoxybibenzyl.[54]
4	1.76	-	373.34	374.10	Myricetin 3,7,3',5'-tetramethyl ether.[55]
5	2.07	275.44	-	274.12	3,4-Dihydroxy-3',5'-dimethoxybibenzyl.[56]

ISSN 2616-0684 (Print)
ISSN 2616-0692 (Electronic)

6	2.95	273.37	-	272.10	4,7-Dihydroxy-2,6-dimethoxy-9,10-dihydrophenanthrene.[57]
7	6.33	443.48	-	442.08	(-)-Epicatechin 3-O-gallate.[58]
8	7.42	335.45	-	334.14	2,3-Dihydroxy-3',4,4',5-tetramethoxybibenzyl.[59]
9	8.13	315.41	-	314.07	Kumatakenin.[60]
10	9.25	317.43	-	316.13	2-Hydroxy-3,4,6,7-tetramethoxy-9,10-dihydrophenanthrene. [61]
11	9.35	317.42	-	316.13	3-Hydroxy-2,4,6,7-tetramethoxy-9,10-dihydrophenanthrene. [62]
12	11.34	333.45	-	332.12	Quadrangularic acid L.[63]
13	14.22	349.45	-	348.39	Schizonepetoside E. [64]
14	15.27	451.60	-	450.31	Erythrophyllic acid.[65]
15	18.08	317.38	-	316.13	3'-Hydroxy-3,4,4'5-tetramethoxystilbene.[66]
16	19.98	301.30	-	300.06	Isokaempferide.[67]
17	20.96	433.75	-	432.10	Vitexin.[68]

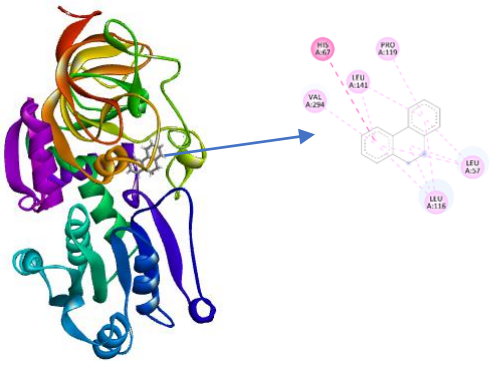

ADH - 9,10-Dihydrophenanthrene

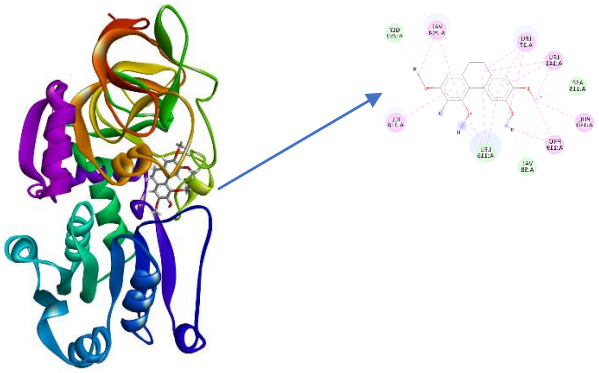

ADH - 3-Hydroxy-2,4,6,7-tetramethoxy-9,10-dihydrophenanthrene

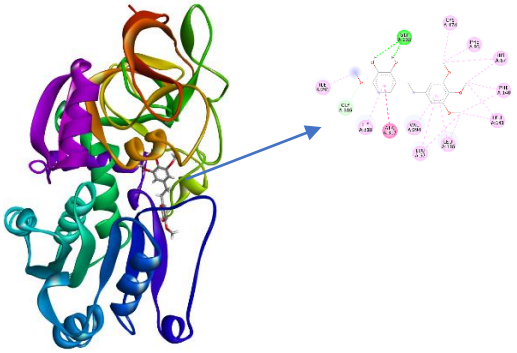

ADH - 2,3-Dihydroxy-3',4,4',5-tetramethoxybibenzyl

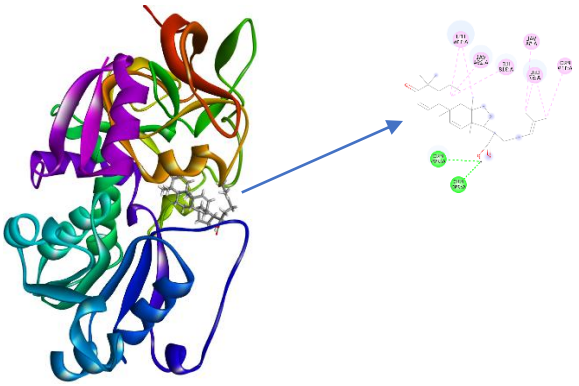

ADH - Erythrophyllic acid

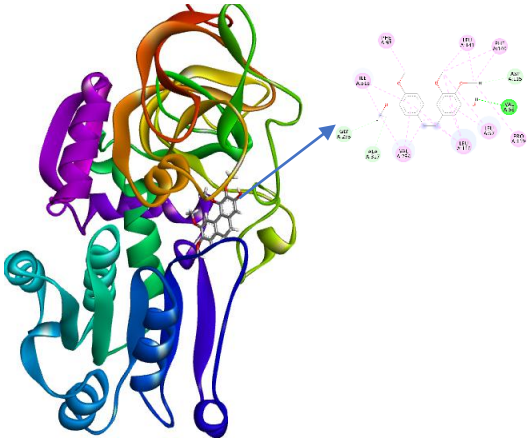

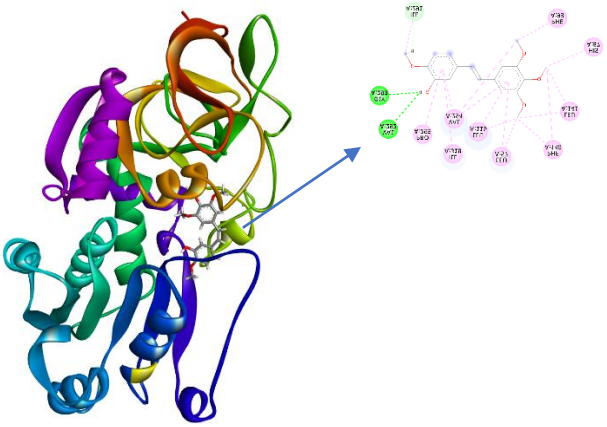

ISSN 2616-0684 (Print)
ISSN 2616-0692 (Electronic)

ADH-2-Hydroxy-3,4,6,7- tetramethoxy-9,10-dihydrophenanthrene ADH - 3'-Hydroxy-3,4,4'5-tetramethoxystilbene

Figure 4: The 3D conformation and 2D view of each ligand-receptor complex

Table 2: ADME Profile of selected compounds from *Combretum indicum* var B seeds

Pubchem CID	Lipinski's rule				HIA	HO
	H (-)	H (+)	MLog P	M		
13058	0	0	5	180.09	0.9944	0.8714
135716	6	2	2	334.14	0.8912	0.5143
14049975	5	1	2	316.13	0.9783	0.6571
162956118	5	1	2	316.13	0.9892	0.6286
100952818	3	1	6	450.31	0.9946	0.5286
5351344	5	1	2	316.13	0.9904	0.7

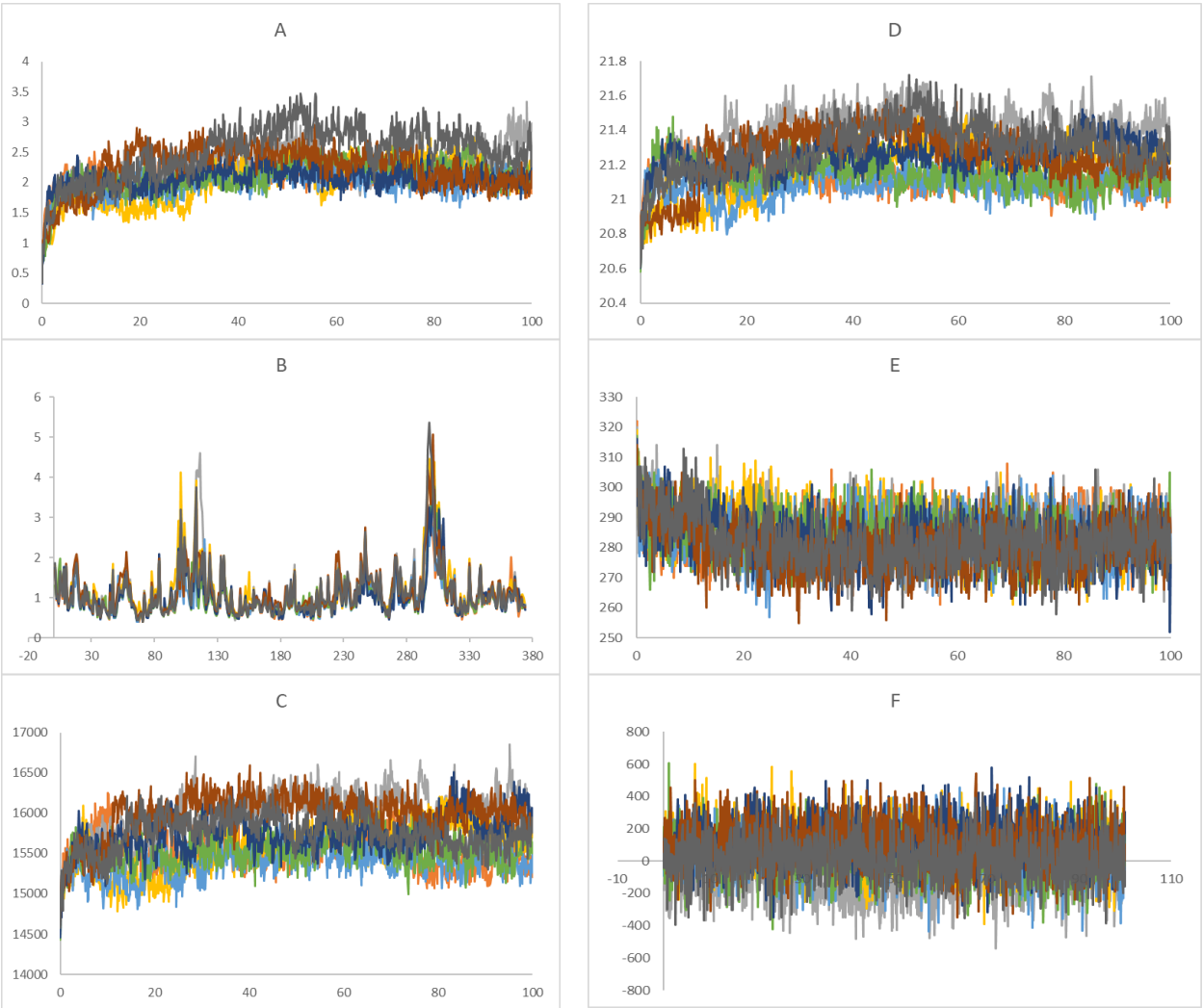

Figure 5: Molecular dynamic simulation for 100 ns. A: RSMD Cα, B: RMSF, C: SASA, D: Rg, E: Hydrogen bond, F: Binding energy

* Orange colour is enzyme, gray: enzyme-fomepizole, yellow: enzyme-9,10-Dihydrophenanthrene, blue: enzyme- 2,3-Dihydroxy-3',4,4',5-tetramethoxybibenzyl, green: enzyme-2-Hydroxy-3,4,6,7- tetramethoxy-9,10-dihydrophenanthrene, purple: enzyme-3-Hydroxy-2,4,6,7-tetramethoxy-9,10-dihydrophenanthrene, red: enzyme-Erythrophyllic acid, black: enzyme- 3'-Hydroxy-3,4,4'5-tetramethoxystilbene.

Rg showed the cohesiveness of the protein molecule, with higher values, indicating a more complex protein molecule.[39] The alcohol dehydrogenase enzyme during a 100 ns simulation had an Rg value of 21.13 Å. The Rg value increased on interaction with the ligands except for the interaction with 9,10-Dihydrophenanthrene, which showed a decreased Rg value of 21.077 Å (Figure 5D).

Hydrogen bonds describe the hydrogen bonding of proteins when interacting with ligands. The higher the hydrogen bonds, the greater the stability of the complex formed.[40] In this study, the initial Hydrogen bond value of the enzyme was 284.296 during the 100 ns simulation (Figure 5E). Hydrogen bond values decreased when the enzyme binds to 3-Hydroxy-2,4,6,7- tetramethoxy-9,10-dihydrophenanthrene (282.194), Erythrophyllic acid (280.136), and 3'-

ISSN 2616-0684 (Print)
ISSN 2616-0692 (Electronic)

Hydroxy-3,4,4'5-tetramethoxystilbene (281.807), whereas Hydrogen bonds increased on enzyme binding to fomepizole (285.605), 9,10-Dihydrophenanthrene (285.342), 2,3-Dihydroxy-3',4,4',5-tetramethoxybibenzyl (285.758), and 2-Hydroxy-3,4,6,7-tetramethoxy-9,10-dihydrophenanthrene (285.758).

The binding energy was calculated using the Poisson–Boltzmann method (PBS), where a more positive value indicated a more potent ligand and enzyme complex.[29] The enzyme and fomepizole complex had a binding energy of -101.485 kJ/mol as an initial value. The binding energy increased in the enzyme - 3'-Hydroxy-3,4,4'5-tetramethoxystilbene complex (11.279 kJ/mol), enzyme - 2,3-Dihydroxy-3',4,4',5-tetramethoxybibenzyl complex (38.317 kJ/mol), enzyme - 2-Hydroxy-3,4,6,7- tetramethoxy-9,10-dihydrophenanthrene complex (43.522 kJ/mol), enzyme - 9,10-Dihydrophenanthrene complex (94.717 kJ/mol), enzyme - Erythrophyllic acid complex (111.231 kJ/mol), and was highest in the enzyme - 3-Hydroxy-2,4,6,7-tetramethoxy-9,10-dihydrophenanthrene complex (135.459 kJ/mol) (Figure 5F). These six compounds show good stability when bound to the alcohol dehydrogenase enzyme, with better binding energy than fomepizole as the positive control ligand.

The FDA approved fomepizole as an inhibitor of alcohol dehydrogenase in ethylene glycol poisoning in 1997 and in methanol poisoning in 2000.[41] Fomepizole was found to be a non-specific ADH inhibitor that prevents methanol and ethylene glycol poisoning. ADH also plays an essential role in the metabolism of several drugs and metabolites containing the alcohol functional group, such as abacavir, hydroxyzine and ethambutol.[42] In a previous study, it was shown that the use of ranitidine and cimetidine increased blood alcohol levels. This is because the two drugs inhibited the action of ADH, preventing the metabolism of alcohol.[43] Bismuth subcitrate is a non-competitive ADH inhibitor with a tetramer dissociation mechanism through interference with the active site of Zn. So Zn was involved in the docking because Zn has a role in serving as a catalyst in the reaction.[44,45]

$C_2H_4(OH)_2 + NAD^+ \rightarrow HOCH_2{-}CHO + NADH + H^+$

Studies on alcohol dehydrogenase inhibitors included H2 receptor blockers (ranitidine and cimetidine), which were shown to inhibit class IV ADH in the stomach, leading to elevated alcohol levels.[46] The use of ranitidine was also shown to reduce the toxicity of methanol,[47] while omeprazole and lansoprazole showed no effect on alcohol metabolism.[48] The use of bismuth subcitrate have be shown to inhibit the action of ADH.[49] Similarly, the formamide group of compounds such as N-Cyclohexylformamide, N-Formylpiperidine, N-Formylpiperidine, N-1-Methylheptylformamide, N-CyclopentylN-cyclopropylformamide and (1S,3R)-3-Butylthiolane l-oxide have been shown to have the ability to act as non-competitive inhibitors of alcohol dehydrogenase.[50] A study have also shown the ability of Cinnamon extract to inhibit alcohol dehydrogenase, with cinnamaldehyde predicted as the potentially active compound.[51] The mechanism of the above alcohol dehydrogenase inhibitors was non-competitive, unlike fomepizole, which is a competitive inhibitor of alcohol dehydrogenase. Therefore, an *in silico* study was designed to predict the stability of the interaction of ligands present in *Combretum indicum* var. B seeds with alcohol dehydrogenase at its active site. This study used molecular docking to identify six compounds; 3'-Hydroxy-3,4,4'5-tetramethoxystilbene, 9,10-Dihydrophenanthrene, 2,3-Dihydroxy-3',4,4',5-tetramethoxybibenzyl, 3-Hydroxy-2,4,6,7-tetramethoxy-9,10-dihydrophenanthrene, 2-Hydroxy-3,4,6,7-tetramethoxy-9,10-dihydrophenanthrene, and Erythrophyllic acid as potential inhibitors of ADH with the PHE93 residue at the enzyme active site crucial in the binding of these ligands.[52]

Conclusion

Results from the present study showed that six compounds from the seeds of *Combretum indicum* var. B have potential as alcohol dehydrogenase inhibitors. These compounds exhibited good stability on binding to alcohol dehydrogenase, with binding energy comparable to fomepizole used as a positive control ligand. However, this study was limited to *in silico* model, necessitating further *in vitro* studies to determine the IC_{50} values of these ligands as well as their inhibition kinetics.

Conflict of Interest

The authors declare no conflict of interest.

Authors' Declaration

The authors hereby declare that the work presented in this article is original and that any liability for claims relating to the content of this article will be borne by them.

Table 3: Binding interactions of docked ligands with ADH enzyme

Pubchem CID	Binding energy (kcal/mol)	Dissociation constant (pM)	Bond type and spacing (Å)	
			Hydrogen	Hydrophobic
3406 (fomepizole)	-3.59	2350000128		UNL1 - LEU116 (4.11), UNL1 - LEU141 (4.31), CYS174 - UNL1 (4.32)
13058 (9,10-Dihydrophenanthrene)	-6.54	16110000		HIS67 - UNL1 (5.69), LEU57 - UNL1 (4.17), LEU116 - UNL1 (4.31), UNL1 - PRO119 (5.11), UNL1 - LEU141 (5.21), UNL1 - VAL294 (5.44)
135716 (2,3-Dihydroxy-3',4,4',5-tetramethoxybibenzyl)	-6.65	13450000	UNL1- GLY293O (1.93), GLY316 - UNL1 (1.88)	UNL1 - LEU57 (4.05), UNL1 - LEU116 (3.88), UNL1 - LEU141 (4.49), UNL1- CYS174 (4.01), UNL1 - ILE291 (3.78), HIS67 - UNL1 (4.17), PHE93 - UNL1(3.68), PHE140 - UNL1 (4.51), UNL1 - VAL294 (4.3),

 ISSN 2616-0684 (Print)
ISSN 2616-0692 (Electronic)

				UNL1 - ILE318 (5.19)
14049975 (2-Hydroxy-3,4,6,7-tetramethoxy-9,10-dihydrophenanthrene)	-7.28	4630000	UNL1 - VAL58 (2.11), UNL1 - ALA317 (2.69), UNL1 - GLY293 (2.61), UNL1 - ASP115 (2.64)	LEU116 - UNL1 (5.23), VAL294 - UNL1 (4.42), UNL1 - ILE318 (4.62), UNL1 - PRO119 (4.37), UNL1 - LEU141 (4.72), UNL1 - LEU57 (4.44), UNL1 - LEU141 (4.17), PHE93 - UNL1 (4.21), PHE140 - UNL1 (4.66), UNL1 - LEU116 (4.24), UNL1 - VAL294 (3.72)
162956118 (3-Hydroxy-2,4,6,7-tetramethoxy-9,10-dihydrophenanthrene)	-7.07	6620000	UNL1 - ASP115 (2.37), UNL1 - VAL58 (2.64), UNL1 - LEU116 (3.02), UNL1 - GLY293 (2.54)	LEU57 - UNL1 (4.31), LEU116 - UNL1 (4.11), LEU141 - UNL1 (4.91), UNL1 - PRO119 (4.04), UNL1 - VAL294 (3.68), PHE140 - UNL1 (4.81), UNL1 - ILE318 (5.18)
100952818 (Erythrophyllic acid)	-7.52	3100000	UNL1 - PRO295 (2.54)	LEU116 - UNL1 (4.57), VaL294 - UNL1 (4.07), ILE318 - UNL1 (5.16), UNL1 - LEU57 (5.02), UNL1 - PRO119 (3.94), UNL1 - VAL58 (4.71)
5351344 (3'-Hydroxy-3,4,4'5-tetramethoxystilbene)	-5.77	58580000	UNL1 - GLY293O (2.31), UNL1 - ILE291O (2.09)	UNL1 - ILE291 (3.88), UNL1 - LEU57 (4.21), UNL1 - LEU116 (4.56), UNL1 - LEU141 (4.36), UNL1 - VAL294 (5.35), HIS67 - UNL1 (3.48), PHE93 - UNL1 (4.78), PHE140 - UNL1 (4.53), UNL1 - PRO295 (5.11), UNL1 - ILE318 (5.23)

Acknowledgements

The authors are grateful to DRTPM for funding this study with Master Contract: 130/E5/PG.02.00.PL/2023, and Derivative Contract: 576/UN8.2/PG/2023

References

1. Kellum JA, Romagnani P, Ashuntantang G, Ronco C, Zarbock A, Anders HJ. Acute kidney injury. Nat Rev Dis Prim. 2021;7(1):52-59.
2. Saied AA, Metwally AA, Dhama K. Gambian children's deaths due to contaminated cough syrups are a mutual responsibility. International journal of surgery (London, England). United States; 2023;109(2):115–116.
3. Ministry of Health of the Republic of Indonesia. Treatment and clinical management of atypical progressive acute kidney anjury in children in health care facilities. 2023.
4. National Agency of Drug and Food Control. Handbook series handling cases of ethylene glycol and diethylene glycol contamination in medicinal syrups. Jakarta. BPOM RI. Jakarta; 2023.
5. Harris JM. Poly(ethylene glycol) chemistry: Biotechnical and biomedical applications. Springer US; 2013. (Topics in Applied Chemistry).
6. Perazella MA, Shirali AC. Nephrotoxicity of cancer immunotherapies: past, present and future. J Am Soc Nephrol. 2018;29(8):2039–2052.
7. Rietjens SJ, de Lange DW, Meulenbelt J. Ethylene glycol or methanol intoxication: which antidote should be used, fomepizole or ethanol? neth. J Med. 2014;72(2):73–79.
8. Brazzelli M, Aucott L, Aceves-Martins M, Robertson C, Jacobsen E, Imamura M, Poobalan A, Manson P, Scotland G, Kaye C, Sawhney S, Boyers D. Biomarkers for assessing acute kidney injury for people who are being considered for admission to critical care: a systematic review and cost-effectiveness analysis. Health technology assessment (Winchester, England). England; 2022;26(7):1–286.
9. Kumar S, Singh J, Dubey A. Valuation of hepatoprotective, antioxidant and cardioprotective effects of aerial part of Quisqualis indica linn in rats. ijrar. 2020;07(1):2020-2027.
10. Adebisi I, Ugwah-Oguejiofor C. In vivo hepatoprotective effect of combretum micranthum leave extract. FASEB J. 2021;35(1):2288-2296.
11. Parusnath M, Naidoo Y, Singh M, Kianersi F, Dewir YH. Antioxidant and antibacterial activities of the leaf and stem

extracts of Combretum molle (R. Br. ex G. Don.) Engl. & Diels. Plants (Basel, Switzerland). 2023;12(9):1757-1773.
12. Peter I, Aroh C, Shere U, Ani N, Adaka I, Asogwa K, Isiogugu O, Abonyi C, Onwuka A. Pharmacological actions of methanol leaf extract of Combretum paniculatum Vent. (Combretaceae) on the gastrointestinal system. Trop J Nat Prod Res. 2020;4(1):270–275.
13. Rajalingam D, Ramachandran V, Subramani P. Evaluation of hepatoprotective and antioxidant effect of Combretum albidum G. Don against CCL4 induced hepatotoxicity in rats. Int J Pharm Pharm Sci. 2016;8(1):218-225.
14. Ujowundu F, Ogugua V, Cosmas U, Nwaoguikpe R. Aqueous extract of Combretum dolichopentalum leaf - a potent inhibitor of carbon tetrachloride induced hepatotoxicity in rats. J Appl Pharm Sci. 2011;1(1):114–121.
15. Sini M, Nwodo OF., Alumanah EO. Hepatoprotective activity of aqueous extract of Combretum sericeum roots against paracetamol induced hepatic damage in rats. 2017;4(1):40–46.
16. Park JH, Hwang MH, Cho YR, Hong SS, Kang JS, Kim WH, Yang SH, Seo DW, Oh JS, Ahn EK. Combretum quadrangulare extract attenuates atopic dermatitis-like skin lesions through modulation of mapk signaling in BALB/c mice. Molecules. 2020;25(8):3390-3404.
17. Idoh K, Dosseh K, Kpatcha T, Agbonon A, Gbeassor M. Protective effect of Combretum Hypopilinum diels: root bark extract against CCl4-Induced hepatotoxicity in wistar rats. Pharmacognosy Res. 2018:10(1):325–331.
18. Dao TBN, Nguyen TMT, Nguyen VQ, Tran TMD, Tran NMA, Nguyen CH, Nguyen HH, Sichaem J, Tran CL, Duong TH. Flavones from Combretum quadrangulare growing in Vietnam and their alpha-glucosidase inhibitory activity. Molecules. 2021;26(9):2531-2545.
19. Suganya S, Schneider L, Nandagopal B. Molecular docking studies of potential inhibition of the alcohol dehydrogenase enzyme by phyllanthin, hypophyllanthin and gallic acid. Crit Rev Eukaryot Gene Expr. 2019;29(4):287–294.
20. Huang X, Zhang S, Li Y, Yang X, Li N, Zeng G, Chen F, Tuo X. Insight into the binding characteristics of rutin and alcohol dehydrogenase: based on the biochemical method, spectroscopic experimental and molecular model. J Photochem Photobiol B Biol. 2022;228(1):394-408.
21. Bisht N, Dalal V, Tewari L. Molecular modeling and dynamics simulation of alcohol dehydrogenase enzyme from high efficacy cellulosic ethanol-producing yeast mutant strain Pichia kudriavzevii BGY1-γm. J Biomol Struct Dyn. 2022;40(22):12022–12036.
22. Haghighi O, Moradi M. In silico study of the structure and ligand interactions of alcohol dehydrogenase from Cyanobacterium Synechocystis Sp. PCC 6803 as a Key Enzyme for Biofuel Production. Appl Biochem Biotechnol. 2020;192(4):1346–1367.
23. Piano MR. Alcohol's effects on the cardiovascular system. Alcohol Res. 2017;38(2):219–241.
24. Hiranuma N, Park H, Baek M, Anishchenko I, Dauparas J, Baker D. Improved protein structure refinement guided by deep learning based accuracy estimation. Nat Commun [Internet]. 2021;12(1):1340-1353.
25. Shanmugavelan R, Musthafa M M. Pharmacokinetics and molecular docking study of siddha polyherbal preparation shailam against covid-19 mutated s gene. Trop J Nat Prod Res. 2022;6(4):502–513.
26. Rahim F, Putra PP, Ismed F, Putra AE, Lucida H. Molecular dynamics, docking and prediction of absorption, distribution, metabolism and excretion of lycopene as protein inhibitor of Bcl2 and DNMT1. Trop J Nat Prod Res. 2023;7(7):3439–3444.
27. O. Olatayo A, D.V. Ayansina A, O. Dahunsi S. Antibacterial activity and molecular docking analysis of the stem bark extracts of Persea americana Mill (Lauraceae). Trop J Nat Prod Res. 2022;6(6):980–990.
28. Morris GM, Huey R, Lindstrom W, Sanner MF, Belew RK, Goodsell DS, Olson AJ. AutoDock4 and AutoDockTools4: Automated docking with selective receptor flexibility. J Comput Chem. 2009;30(16):2785–2791.
29. Chen DE, Willick DL, Ruckel JB, Floriano WB. Principal component analysis of binding energies for single-point mutants of hT2R16 bound to an agonist correlate with experimental mutant cell response. J Comput Biol a J Comput Mol cell Biol. 2015;22(1):37–53.
30. Falodun A, Siraj R, Choudhary M. GC-MS Analysis of insecticidal leaf essential oil of Pyrenacantha staudtii Hutch and Dalz (Icacinaceae). Trop J Pharm Res.2009;8(2);22-30.
31. Land H, Humble MS. YASARA: A Tool to obtain structural guidance in biocatalytic investigations. Methods Mol Biol. 2018;1685(1):43–67.
32. Beaulieu J, Roberts DM, Gosselin S, Hoffman RS, Lavergne V, Hovda KE, Megarbane B, Lung D, Thanacoody R, Ghannoum M. Treating ethylene glycol poisoning with alcohol dehydrogenase inhibition, but without extracorporeal treatments: a systematic review. Clin Toxicol (Phila). 2022;60(7):784–797.
33. Seo JW, Lee JH, Son IS, Kim YJ, Kim DY, Hwang Y, Chung HA, Choi HS, Lim SD. Acute oxalate nephropathy caused by ethylene glycol poisoning. Kidney Res Clin Pract. 2012;31(4):249–252.
34. Okolie NP, Falodun A, Davids O. Evaluation of the antioxidant activity of root extract of pepper fruit (Dennetia tripetala), and it's potential for the inhibition of lipid peroxidation. African J Tradit Complement Altern Med AJTCAM. 2014;11(3):221–227.
35. Shekhawat PB, Pokharkar VB. Understanding peroral absorption: regulatory aspects and contemporary approaches to tackling solubility and permeability hurdles. Acta Pharm Sin B. 2017;7(3):260–280.
36. Tran QH, Nguyen QT, Vo NQH, Mai TT, Tran TTN, Tran TD, Lie MT, Trinh DH, Thai KM. Structure-based 3D-pharmacophore modeling to discover novel interleukin 6 inhibitors: An *in silico* screening, molecular dynamics simulations and binding free energy calculations. PLoS One [Internet]. 2022;17(4):632-646.
37. Liu K, Watanabe E, Kokubo H. Exploring the stability of ligand binding modes to proteins by molecular dynamics simulations. J Comput Aided Mol Des. 2017;31(2):201–211.
38. Martínez L. Automatic identification of mobile and rigid substructures in molecular dynamics simulations and fractional structural fluctuation analysis. PLoS One. 2015;10(3):264-274.
39. Lobanov MI, Bogatyreva NS, Galzitskaia O V. Radius of gyration is indicator of compactness of protein structure. Mol Biol (Mosk). 2008;42(4):701–706.
40. Rahman MM, Saha T, Islam KJ, Suman RH, Biswas S, Rahat EU, Hossen MR, Islam R, Hossain MN, Mamun AA, Khan M, Ali MA, Halim MA. Virtual screening, molecular dynamics and structure-activity relationship studies to identify potent approved drugs for Covid-19 treatment. J Biomol Struct Dyn. 2021;39(16):6231–41.
41. Mégarbane B. Treatment of patients with ethylene glycol or methanol poisoning: focus on fomepizole. Open Access Emerg Med. 2010;2(1):67–75.
42. Di L, Balesano A, Jordan S, Shi SM. The role of alcohol dehydrogenase in drug metabolism: beyond ethanol oxidation. AAPS J. 2021;23(1):20-34.
43. Luo ML, Chen H, Chen GY, Wang S, Wang Y, Yang FQ. Preparation of alcohol dehydrogenase–zinc phosphate hybrid nanoflowers through biomimetic mineralization and its application in the inhibitor screening. Molecules. 2023;28(1):5429-5445.

44. Plapp B V, Savarimuthu BR, Ferraro DJ, Rubach JK, Brown EN, Ramaswamy S. Horse Liver alcohol dehydrogenase: zinc coordination and catalysis. Biochemistry. 2017;56(28):3632–3646.
45. Zhang X, Zhang B, Lin J, Wei D. Oxidation of ethylene glycol to glycolaldehyde using a highly selective alcohol dehydrogenase from gluconobacter oxydans. J Mol Catal B Enzym. 2015;112(1):69–75.
46. Jelski W, Orywal K, Szmitkowski M. Effects of H2-blockers on alcohol dehydrogenase (ADH) activity. Pol Merkur Lekarski. 2008;25(5):531–534.
47. El-Bakary AA, El-Dakrory SA, Attalla SM, Hasanein NA, Malek HA. Ranitidine as an alcohol dehydrogenase inhibitor in acute methanol toxicity in rats. Hum Exp Toxicol. 2010;29(2):93–101.
48. van der Zalm IJB, Tobé TJM, Logtenberg SJJ. Omeprazole-induced and pantoprazole-induced asymptomatic hyponatremia: a case report. J Med Case Rep. 2020;14(1):83-87.
49. Keogan DM, Griffith DM. Current and potential applications of bismuth-based drugs. Molecules. 2014;19(9):15258–15297.
50. Kohlmeyer C, Schäfer A, Huy PH, Hilt G. Formamide-catalyzed nucleophilic substitutions: mechanistic insight and rationalization of catalytic activity. ACS Catal. 2020;10(19):11567–11577.
51. Do J, In MJ, Kim DC. Inhibitory effect of cinnamon (Cinnamomum cassia Presl) extract and cinnamaldehyde on alcohol dehydrogenase. J Appl Biol Chem. 2022;65(3):183−187.
52. Lee SL, Lee YP, Wu ML, Chi YC, Liu CM, Lai CL, Yin SJ. Inhibition of human alcohol and aldehyde dehydrogenases by aspirin and salicylate: assessment of the effects on first-pass metabolism of ethanol. Biochem Pharmacol. 2015;95(1):71–79.
53. Pettit G, Singh S, Niven M, Schmidt J. Cell growth inhibitory dihydrophenanthrene and phenanthrene constituents of the african tree Combretum caffrum. Can J Chem. 2011;66(1):406–413.
54. Yang J, Jiang J, Wang W, Zhang Y, Liu Y, Chen Y. Isolation and characterization of batatasin iii and 3,4 ’-dihydroxy-5-methoxybibenzyl: a pair of positional isomers from sunipia scariosa. Trop J Pharm Res. 2014;13(1):533–538.
55. Zhang Y, Yan G, Sun C, Li H, Fu Y, Xu W. Apoptosis effects of dihydrokaempferol isolated from Bauhinia championii on synoviocytes. Evid Based Complement Alternat Med. 2018;18(4):6160-6170.
56. Putri HE, Sritularak B, Chanvorachote P. DS-1 Inhibits migration and invasion of non-small-cell lung cancer cells through suppression of epithelial to mesenchymal transition and integrin β1/FAK signaling. Anticancer Res. 2021;41(6):2913–2923.
57. Duangprompo W, Aree K, Itharat A, Hansakul P. Effects of 5,6-dihydroxy-2,4-dimethoxy-9,10-dihydrophenanthrene on G(2)/M cell cycle arrest and apoptosis in human lung carcinoma cells. Am J Chin Med. 2016;44(7):1473–1490.
58. Almatroodi SA, Almatroudi A, Khan AA, Alhumaydhi FA, Alsahli MA, Rahmani AH. Potential therapeutic targets of epigallocatechin gallate (egcg), the most abundant catechin in green tea, and its role in the therapy of various types of cancer. Molecules. 2020;25(1):3146-3185.
59. Saeed BMS, Al-Jadaan SAN, Abbas BA. Study on anticancer activity of 4, 4’-[1,4-phenylenebis(1,3,4-thiadiazole-5,2-diyl)] bis (azaneylylidene) bis (methaneylylidene) diphenolon breast cancer cells. Arch Razi Inst. 2021;76(4):821–827.
60. Woo JH, Ahn JH, Jang DS, Lee KT, Choi JH. Effect of kumatakenin isolated from cloves on the apoptosis of cancer cells and the alternative activation of tumor-associated macrophages. J Agric Food Chem. 2017;65(36):7893–7899.
61. Silén H, Salih EYA, Mgbeahuruike EE, Fyhrqvist P. Ethnopharmacology, antimicrobial potency, and phytochemistry of african combretum and pteleopsis species (combretaceae): a review. Antibiotics. 2023;12(2):264-316.
62. Śliwiński T, Kowalczyk T, Sitarek P, Kolanowska M. Orchidaceae-derived anticancer agents: a review. Cancers (Basel). 2022;14(3):754-785.
63. Sundaran J, Begum R, Vasanthi M, Kamalapathy M, Bupesh G, Sahoo U. A short review on pharmacological activity of Cissus quadrangularis. Bioinformation. 2020;16(8):579–585.
64. Forid MS, Rahman MA, Aluwi MFFM, Uddin MN, Roy TG, Mohanta MC, Huq AM, Zakaria ZA. Pharmacoinformatics and UPLC-QTOF/ESI-MS-based phytochemical screening of Combretum indicum against oxidative stress and alloxan-induced diabetes in long-evans rats. Molecules. 2021;26(15);4634-4664.
65. Mawoza T, Ndove T. Combretum erythrophyllum (Burch.) Sond. (Combretaceae): a review of its ethnomedicinal uses, phytochemistry and pharmacology. Glob J Biol Agric Heal Sci. 2015;4(1):105–109.
66. Nowicki A, Skupin-Mrugalska P, Jozkowiak M, Wierzchowski M, Rucinski M, Ramlau P, Krajka-Kuzniak V, Jodynis-Liebert J, Piotrowska-Kempisty H. The Effect of 3’-hydroxy-3,4,5,4’-tetramethoxy -stilbene, the metabolite of the resveratrol analogue dmu-212, on the motility and proliferation of ovarian cancer cells. Int J Mol Sci. 2020;21(3);1100-1116.
67. Kim BG. Biosynthesis of bioactive isokaemferide from naringenin in Escherichia coli. J Appl Biol Chem. 2019;62(1):1–6.
68. Bhardwaj M, Cho HJ, Paul S, Jakhar R, Khan I, Lee SJ, Kim BY, Krishnan M, Khaket TP, Lee HG, Kang SC. Vitexin induces apoptosis by suppressing autophagy in multi-drug resistant colorectal cancer cells. Oncotarget. 2018;9(3):3278–3291.